ELSEVIER

www.elsevier.nl/locate/jorganchem

Journal of Organometallic Chemistry 589 (1999) 213–221

Journal of Organometallic Chemistry

Double addition of a 1,3-diyne to C_2 on an Ru_5 cluster gives a multi-branched C_{10} chain

Chris J. Adams [a], Michael I. Bruce [a,*], Brian W. Skelton [b], Allan H. White [b]

[a] *Department of Chemistry, University of Adelaide, Adelaide 5005, Australia*
[b] *Department of Chemistry, University of Western Australia, Nedlands 6907, Australia*

Received 5 June 1999

Abstract

Reactions of the dicarbon-containing complex $Ru_5(\mu_5\text{-}C_2)(\mu\text{-}SMe)_2(\mu\text{-}PPh_2)_2(CO)_{11}$ (**1**) with 1,4-diphenylbuta-1,3-diyne gave as the major products $Ru_5\{\mu_5\text{-}CCCPhC(C{\equiv}CPh)\}(\mu_3\text{-}SMe)(\mu\text{-}SMe)(\mu\text{-}PPh_2)_2(CO)_n$ ($n = 11$ (**6**), 9 (**8**)) and $Ru_5\{\mu_5\text{-}CCC(C{\equiv}CPh)CPh\}(\mu\text{-}PPh_2)_2(\mu\text{-}SMe)_2(CO)_{10}$ (**7**), thermolysis of the latter also giving **8**. Minor products were characterised as $Ru_5\{\mu_5\text{-}CC(SMe)C(C{\equiv}CPh)CPh\}(\mu\text{-}PPh_2)_2(\mu\text{-}SMe)(CO)_{10}$ (**9**) (two isomers) and $Ru_5\{\mu_4\text{-}CC[C(C{\equiv}CPh)CPh]C(C{\equiv}CPh)CPh\}(\mu\text{-}PPh_2)_2(\mu_3\text{-}SMe)_2(CO)_8$ (**10**). The structures of **8**, **9** and **10** were determined from single-crystal X-ray studies; **8** and **10** have 80 cluster valence electrons, two more than the expected number for an M_5 cluster with six M–M bonds. Each has two Ru–Ru separations in excess of 3.0 Å.

Keywords: 1,3-Diyne; Ruthenium; Clusters; X-ray structures

1. Introduction

Previous papers have described the wide diversity present in products obtained by combination of one or two alkyne molecules with the C_2 ligand in the open pentanuclear cluster $Ru_5(\mu_5\text{-}C_2)(\mu\text{-}SMe)_2(\mu\text{-}PPh_2)_2(CO)_{11}$ (**1**) [1]. Scheme 1 illustrates the four common structural types (**2**–**5**) found for products from reactions between **1** and terminal and internal alkynes, although only two are common to both [2–4]. In closely connected studies we have also been interested in the synthesis and reactions of clusters containing 1,3-diynes, part of which have been directed at using uncoordinated C≡C triple bonds in further interactions with suitable metal substrates as intermediates on the way to larger homo- and heterometallic clusters. The present paper describes the products from reactions between **1** and 1,4-diphenylbuta-1,3-diyne, PhC≡CC≡CPh, among which is a cluster containing an unusual multi-branched C_{10} chain. Some of these results were incorporated into recent summaries of the chemistry of **1** [1].

2. Results

A series of reactions between **1** and PhC≡CC≡CPh were carried out in toluene at 90°C for either 9.5 h (A) or 43 h (B), or at 120° for 12 h (C), conditions established by exploratory experiments as giving the best yields of the five products (see Section 5). The products were isolated from the reaction mixtures by preparative TLC and were characterised by elemental analyses and the usual spectroscopic methods (Table 1).

A red fraction was obtained in a 5% yield from reaction B and determined to be $Ru_5\{\mu_5\text{-}CCCPhC(C{\equiv}CPh)\}(\mu_3\text{-}SMe)(\mu\text{-}SMe)(\mu\text{-}PPh_2)_2(CO)_{11}$ (**6**), an analogue of products **2** obtained from **1** and C_2Ph_2 [2] or HC≡CR (R = Ph, $SiMe_3$) [3]; the $SiMe_3$ complex has been fully characterised from a single-crystal X-ray study. In this complex, one of the ruthenium atoms has been extruded from the Ru_5 cluster originally present in **1**, but is retained in the complex by virtue of the PPh_2, SMe and organic ligands that form bridges between the Ru_4 core and the fifth metal atom. This structural

* Corresponding author. Tel.: +618-8303-5939; fax: +618-8303-4358.
E-mail address: michael.bruce@adelaide.edu.au (M.I. Bruce)

0022-328X/99/$ - see front matter
PII: S0022-328X(99)00404-0

Table 1
Analytical and spectroscopic data

Compound/analysis	IR ν(CO) [a]	NMR [b]
6 $Ru_5\{\mu_5\text{-}CCC(C{\equiv}CPh)CPh\}(\mu_3\text{-}SMe)(\mu\text{-}SMe)(\mu\text{-}PPh_2)_2(CO)_{11}$ Anal. Found: C, 44.05; H, 2.50. $C_{55}H_{36}O_{11}P_2Ru_5S_2$ Calc.: C, 43.91; H, 2.41; M, 1506. FAB MS (m/z): 1506, M^+	2088m, 2039s, 2030m, 2022vs, 2011s, 2006sh, 1977m, 1972sh, 1968m, 1954w, 1943w	^{1}H-NMR: δ 1.18 (3H, s, SMe), 2.20 (3H, d, J_{HP} 3.2 Hz, SMe), 7.06–7.83 (30H, m, Ph)
7 $Ru_5\{\mu_5\text{-}CCC(C{\equiv}CPh)CPh\}(\mu\text{-}SMe)_2(\mu\text{-}PPh_2)_2(CO)_{10}$ Anal. Found: C, 44.18; H, 2.44. $C_{54}H_{36}O_{10}P_2Ru_5S_2$ Calc. C, 43.93; H, 2.46; M, 1476. FAB MS (m/z): 1476, M^+; 1448–1196, $[M\text{–}n\text{CO}]^+$ ($n = 1$–10)	2047m, 2032vs, 2022s, 2010s, 2001m, 1990m, 1986m, 1970m, 1960w, 1956m	^{1}H-NMR: δ 1.63 (3H, s(br), SMe), 2.07 (3H, s, SMe), 6.92–7.93 (30H, m, Ph). ^{13}C-NMR: δ 23.42 (s, SMe), 23.85 (s, SMe), 88.34 (s, C$\equiv$C̲Ph), 93.17 (s, C̲$\equiv$CPh), 124.56 [s, C(C_2Ph)C̲Ph], 125.29–133.31 (m, Ph), 140.78 [d, J_{CP} 37.1 Hz, *ipso* C (PPh)], 142.11 [d, J_{CP} 40.6 Hz, *ipso* C (PPh)], 142.19 [s, *ipso* C (C$\equiv$CPh)], 144.20 [d, J_{CP} 26.0 Hz, *ipso* C (PPh)], 145.68 [d, J_{CP} 26.6 Hz, *ipso* C (PPh)], 151.28 [s, *ipso* C (CPh)], 189.19 [s(br), CO], 191.63 (d, J_{CP} 5.2 Hz, CO), 194.08 (d, J_{CP} 5.4 Hz, CO), 194.23 (s, CO), 194.92 (d, J_{CP} 3.2 Hz, CO), 197.40 (d, J_{CP} 8.2 Hz, CO), 198.52 (s, CO), 198.69 [s, C̲(C_2Ph)CPh], 205.42 (s, CO), 206.11 (s, CO), 258.19 [s, CC̲C(C_2Ph)CPh)], 326.95 [CC̲C(C_2Ph)CPh]
8 $Ru_5\{\mu_5\text{-}CCC(C{\equiv}CPh)CPh\}(\mu_3\text{-}SMe)(\mu\text{-}SMe)(\mu\text{-}PPh_2)_2(CO)_9$ Anal. Found: C, 43.72; H, 2.44. $C_{53}H_{36}O_9P_2Ru_5S_2$ Calc.: C, 43.95; H, 2.51; M, 1448. FAB MS (m/z): 1448, M^+; 1420–1196, $[M\text{–}n\text{CO}]^+$ (n = 1–9)	2042m, 2030s, 2018vs, 2006s, 1980m, 1977m, 1968m, 1945sh, 1939m	^{1}H-NMR: δ 1.41 (3H, d, J_{CP} 2.8 Hz, SMe), 2.49 (3H, d, J_{CP} 2.2 Hz, SMe), 6.88–7.78 (30H, m, Ph). ^{13}C-NMR: δ 17.56 (s, SMe), 27.77 (s, SMe), 85.40 (s, C$\equiv$C̲Ph), 87.90 (s, C̲$\equiv$CPh), 123.07 [s, CC(C_2Ph)C̲Ph], 126.71–135.01 (m, Ph), 135.11 [s, *ipso* C (C$\equiv$CPh)], 140.27 [d, J_{CP} 35.6 Hz, *ipso* C (PPh)], 141.79 [d, J_{CP} 35.3 Hz, *ipso* C (PPh)], 144.71 [d, J_{CP} 33.8 Hz, *ipso* C (PPh)], 147.89 [s, *ipso* C (CPh)], 162.09 [s, CC̲(C_2Ph)CPh], 189.18 [d, J_{CP} 3.5 Hz, CC̲C(C_2Ph)], 192.35 (d, J_{CP} 6.7 Hz, CO), 193.62 (d, J_{CP} 8.5 Hz, CO), 195.12 (d, J_{CP} 8.0 Hz, CO), 195.90 (s, CO), 196.94 (d, J_{CP} 8.5 Hz, CO), 201.04 (s, CO), 201.38 (s, CO), 202.06 (d, J_{CP} 4.9 Hz, CO), 204.62 (d, J_{CP} 10.8 Hz, CO), 208.54 [t, J_{CP} 4.2 Hz, C̲CC(C_2Ph)]
9 $Ru_5\{\mu_5\text{-}CC(SMe)C(C{\equiv}CPh)CPh\}(\mu\text{-}SMe)(\mu\text{-}PPh_2)_2(CO)_{10}$ Anal. Found: C, 43.38; H, 2.41. $C_{54}H_{36}O_{10}P_2Ru_5S_2$ Calc.: C, 43.93; H, 2.46; M, 1476. FAB MS (m/z): 1478, M^+; 1450–1198, $[M\text{–}n\text{CO}]^+$ ($n = 1$–10)	2039m, 2020vs, 2012vs, 1996m, 1979m, 1976sh, 1970m, 1962m, 1948m	^{1}H-NMR: δ 1.74* (0.75H, s, SMe), 2.45* (0.75H, s, SMe), 2.50 (3H, s, SMe), 2.86 (3H, s, SMe), 6.85–7.87 (37.5H, m, Ph). ^{13}C-NMR: δ (CD_2Cl_2) 25.94*, 26.28 (s, SMe), 31.52, 32.08* (s, SMe), 89.36, 89.69* (s, ?), 70.72, 95.25* (d, J_{CP} 6.2, 6.9* Hz, ?), 97.42*, 105.07 (s, ?), 122.70, 125.20* (s, ?), 127.70–133.77 (m, Ph), 137.93 [s, *ipso* C (C$\equiv$CPh)], 139.49 [d, J_{CP} 28.5 Hz, *ipso* C (PPh)], 141.71* [d, J_{CP} 29.0 Hz, *ipso* C (PPh)], 141.73* [s, *ipso* C (C$\equiv$Ph)], 142.52* [d, J_{CP} 38.2 Hz, *ipso* C (PPh)], 142.59 [d, J_{CP} 37.6 Hz, *ipso* C (PPh))] 144.15* [d, J_{CP} 28.2 Hz, *ipso* C (PPh)], 144.18 [d, J_{CP} 23.5 Hz, *ipso* C (PPh)], 144.81* [d, J_{CP} 30.4 Hz, *ipso* C (PPh)], 145.36 [d, J_{CP} 30.4 Hz, *ipso* C (PPh)], 149.03 [s, *ipso* C (CPh)], 181.77 [s, CC̲(C_2Ph)CPh], 191.75 (d, J_{CP} 4.5 Hz, CO), 192.05 (d, J_{CP} 7.5 Hz, CO), 194.38 (d, J_{CP} 8.6 Hz, CO), 194.42 (d, J_{CP} 8.6 Hz, CO), 194.70 (d, J_{CP} 7.8 Hz, CO), 195.08 (d, J_{CP} 8.5 Hz, CO), 196.06 (d, J_{CP} 9.2 Hz, CO), 197.73 (d, J_{CP} 7.7 Hz, CO), 198.26 (d, J_{CP} 2.6 Hz, CO), 198.85 (s, CO), 199.21 (d, J_{CP} 1.5 Hz, CO), 199.32 (s, CO), 199.44 (s, CO), 200.25 (d, J_{CP} 4.5 Hz, CO), 201.64 (s, CO), 201.72 (s, CO), 202.01 (s, CO), 202.65 (d, J_{CP} 2.8 Hz, CO), 203.14 (s, CO), 203.88 (s, CO), 284.96, 288.94* [d, J_{CP} 13.1, 12.1* Hz, C̲CC(C_2Ph)]. *Minor isomer (CO and Ph (excluding *ipso* carbons) resonances for each isomer could not be unambiguously assigned
10 $Ru_5\{\mu_4\text{-}CC\{C(C{\equiv}CPh)CPh\}C(C{\equiv}CPh)\text{-}CPh\}(\mu_3\text{-}SMe)_2(\mu\text{-}PPh_2)_2(CO)_8$ Anal. Found: C, 50.12; H, 3.00. $C_{68}H_{46}O_8P_2Ru_5S_2$ Calc.: C, 50.34; H, 2.86; M, 1624. FAB MS (m/z): 1624, M^+; 1596, $[M\text{–CO}]^+$	2037m, 2019vs, 1993m, 1975(sh), 1971vs, 1963m, 1946m	^{1}H-NMR: δ 1.87 (3H, s, SMe), 2.89 (3H, s, SMe), 6.44–7.48 (30H, m, Ph)

[a] ν(CO) cm^{-1}.
[b] Chemical shifts and coupling constants (Hz).

assignment for **6** is supported by similarities in the IR ν(CO) spectrum, particularly the high-energy absorption at 2088 cm^{-1}, and the ^{1}H-NMR spectrum (SMe resonances at δ 1.18 and 2.20; c.f. δ 1.07 and 2.25 for the C_2Ph_2 analogue). The molecular ion was found at m/z 1506 in the fast-atom bombardment (FAB) mass spectrum.

The brown complex $Ru_5\{\mu_5$-CCC(C≡CPh)CPh$\}(\mu$-SMe$)_2(\mu$-PPh$_2)_2$(CO)$_{10}$ (**7**), isolated in 24–51% yields from all three reactions, was identified by elemental analysis and by comparison of its IR ν(CO) spectra and ^{1}H- and ^{13}C-NMR spectra with those of the crystallographically characterised analogue (**3-Ph**) obtained from the reaction between **1** and C_2Ph_2 [2]. Thus, the overall ν(CO) band patterns are similar and at frequencies within $\pm$2–4 cm^{-1}, while characteristic resonances for the SMe groups occur at δ 1.63 and 2.07 (^{1}H) and at δ 23.42 and 23.85 (^{13}C), which may be compared with values of δ_H 1.68 and 2.16 and δ_c 23.62 and 23.72 found for **3-Ph**. The carbons of the C_4 chain are found at δ 124.56, 198.69, 258.19 and 326.95 (c.f. 159.97, 179.52, 265.13 and 325.81 for **3-Ph**). The FAB mass spectrum contained M^+ at m/z 1476.

The third complex $Ru_5\{\mu_5$-CCC(C≡CPh)CPh$\}(\mu_3$-SMe$)(\mu$-SMe$)(\mu$-PPh$_2)_2$(CO)$_9$ (**8**) was obtained as light brown crystals in ca. 20% yield from all three reactions. In this case, characterisation as a structural analogue of known type **5** previously obtained from **1** and HC≡CPh was achieved by a single-crystal X-ray study [3]. Comparison with **5** shows very similar ν(CO) spectra (nine bands between 2042 and 1939 cm^{-1}), while the NMR spectra contained resonances for the SMe groups at δ 1.41 and 2.49 (^{1}H) and at δ 17.56 and 27.77 (^{13}C), which may be compared with values of δ 1.43 and 2.45 (^{1}H) and 17.71 and 27.70 (^{13}C) found for **5**. The four backbone carbons of the organic ligand were found at δ 123.07, 162.09, 189.18 and 208.54, chemical shifts of three of which are comparable with those for **5** at δ 156.87, 186.86 and 209.54; the terminal carbon C(4) in the latter is at δ 87.97, a difference which can perhaps be ascribed to the different substituents (Ph versus C≡CPh). The FAB mass spectrum contained M^+ at m/z 1448.

Red crystals of $Ru_5\{\mu_5$-CC(SMe)C(C≡CPh)CPh$\}(\mu$-SMe$)(\mu$-PPh$_2)_2$(CO)$_{10}$ (**9**) were obtained in 14–19% yields from these reactions. The X-ray structural determination described below showed that migration of one SMe group to C(2) had occurred to give a thioether ligand. This complex had a satisfactory elemental analysis and gave M^+ at m/z 1476. The NMR spectra showed that two isomers were present in the initial product in ca. 1/4 ratio; the X-ray structure is of the major isomer. The two isomers gave distinct signals in the ^{1}H- and ^{13}C-NMR spectra, the two SMe groups being found at δ 1.74 and 2.45 (minor) and 2.50 and 2.86 (major), 25.94 and 32.08 (minor) and 26.28 and 31.52 (major). The carbons of the C_4 chain are found at

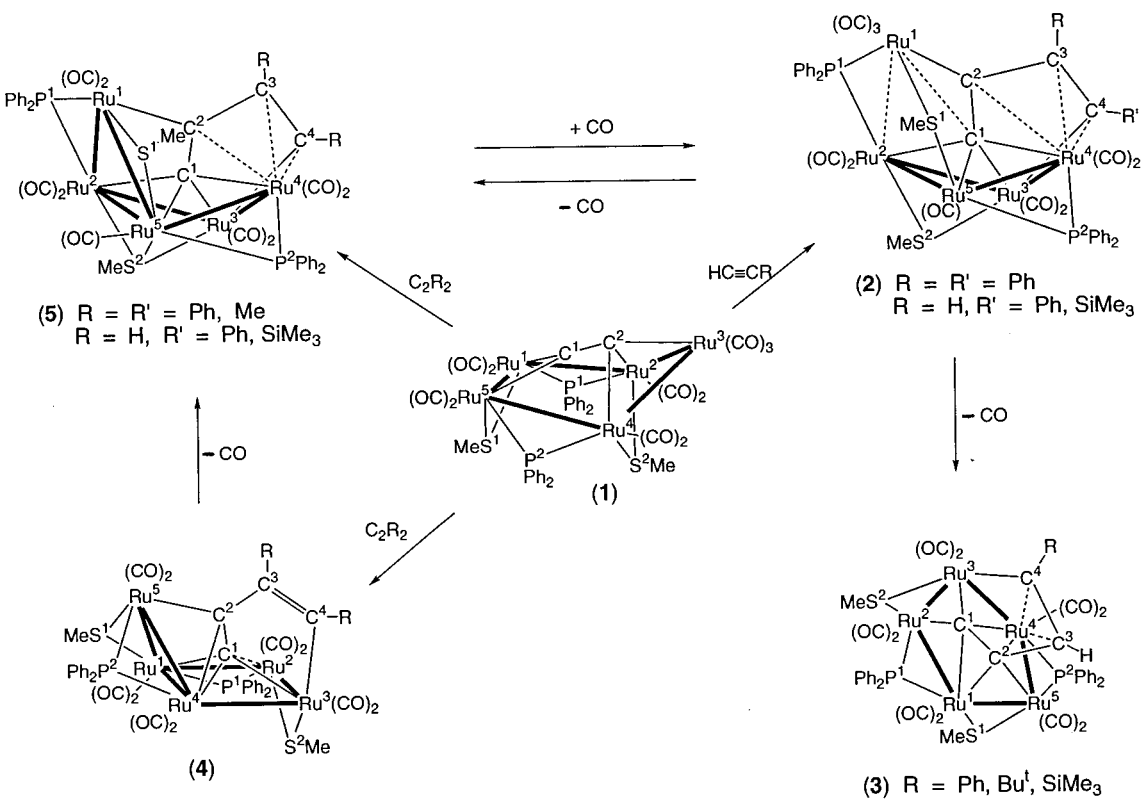

Scheme 1.

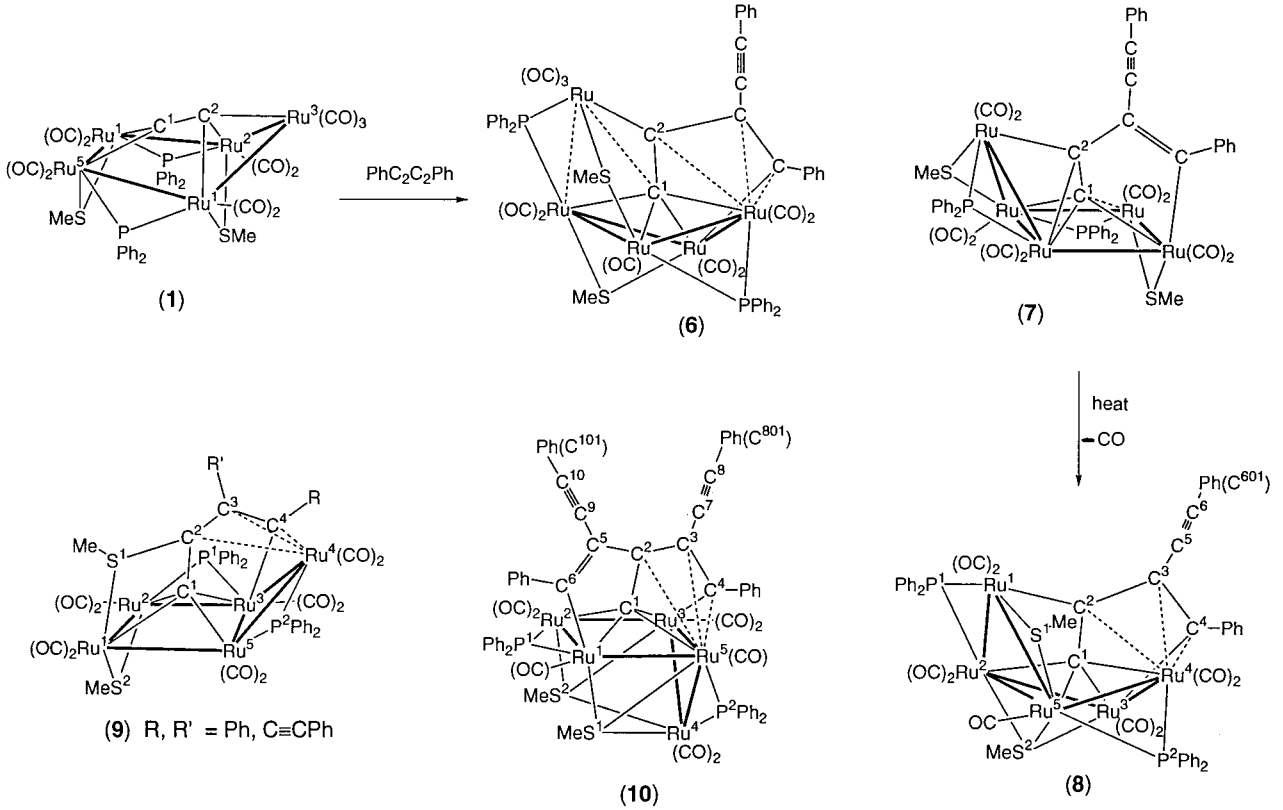

Scheme 2.

δ 105.07, 122.70, 181.77 and 284.96 for the major isomer; the resonances for the minor isomer were not found. These values may be compared to those found for the related derivative $Ru_5\{\mu_5$-CC[C(O)SMe]-CHCPh$\}\mu$-SMe)(μ-$PPh_2)_2(CO)_{10}$ (**11**), for which δ_H values of 1.79 and 2.40 were found for the two SMe groups [3]. It is likely that the two isomers differ in the relative locations of the Ph and C≡CPh groups on C(3) and C(4), as shown in Scheme 2.

The reaction carried out at lower temperatures for an extended period afforded a fifth complex, shown to be $Ru_5\{\mu_4$-CC[C(C≡CPh)CPh]C(C≡CPh)CPh$\}(\mu_3$-$SMe)_2$-(μ-$PPh_2)_2(CO)_8$ (**10**) by a single-crystal X-ray structure determination. This revealed that two diyne molecules have been attached to one carbon of the C_2 fragment in **1**. The FAB mass spectrum contains M^+ at m/z 1624, while the IR ν(CO) spectrum is relatively simple when compared with those of the other complexes described above, containing only seven absorptions between 2037 and 1946 cm^{-1}. The SMe groups appear as two singlets at δ 1.87 and 2.89. In $Ru_5\{\mu_5$-CC[CHC($SiMe_3$)]C[=CH($SiMe_3$)]CO$\}(\mu$-$SMe)_2(\mu$-$PPh_2)_2(CO)_8$ (**12**), where two HC_2SiMe_3 moieties have added to the C_2 unit in **1**, both the IR ν(CO) (seven bands between 2043 and 1945 cm^{-1}) and the ^{1}H-NMR spectra (SMe at δ 1.07, 2.25) have some similarities to those of **10**.

2.1. Molecular structures of **8**, **9** and **10**

Plots of the three molecules are given in Figs. 1–3 and selected structural data are collected in Tables 2 and 3. Crystal data and refinement details are shown in Table 4. The Ru_5 cores in all three complexes have open-envelope conformations. In **8**, the Ru_4 rhombus is bent along the Ru(3)…Ru(5) vector (dihedral angle 39.28(4)°), while the Ru(1,2,5) flap forms a dihedral angle of 73.31(4)° with the Ru(2,3,5) portion. In **9** and **10**, the dihedral angles between the flaps and the Ru_4 rhombus are 56.04(5)/57.92(5) (mols. 1,2) and 87.71(3)°, respectively. The two PPh_2 groups bridge the Ru(1)–Ru(2) and Ru(4)–Ru(5) edges in **8** and **10**, but in **9**, P(1) bridges Ru(2)–Ru(3) (all Ru–P distances range between 2.195 and 2.363(3) Å). One SMe group bridges Ru(1)–Ru(5) and Ru(1)–Ru(2) in **8** and **9**, respectively (Ru–S 2.347(6)–2.412(3) Å). The second SMe group adopts the μ_3-bridging mode in **8** [Ru(2,3,5)–S(2) 2.356–2.471(3) Å), while in **10**, the two SMe groups are each attached to three Ru atoms: Ru(1,4,5)–S(1) are shorter (at 2.361, 2.370 and 2.383(3) Å) than Ru(2,3,4)–S(2) (range between 2.402 and 2.429(3) Å).

The organic ligand in **8** is formed by insertion of one C≡C triple bond into an Ru–C bond of **1**, to give the

four-carbon chain C(1)–C(4). Of this, atom C(1) is more strongly bonded to Ru(2,3) (2.119, 2.077(8) Å) than to Ru(4,5) [2.284, 2.220(8) Å], while atom C(4) is σ-bonded to Ru(3) (2.042(9) Å). All four carbons are bonded as a 1,3-diene to Ru(4) (Ru–C 2.284–2.332(8) Å), so that the C_4Ru_2 unit resembles similar fragments found in simpler systems such as $Ru_2(\mu\text{-}2\eta^1{:}\eta^4\text{-}C_4R_4)(CO)_6$. This complex is thus structurally analogous to several other complexes obtained from reactions between **1** and mono-alkynes, e.g. HC≡CR (R = Ph, $SiMe_3$) [3].

In **9**, the C_2 ligand in **1** has combined with the diyne in a similar manner to that found in **8**. In addition, one of the SMe groups has migrated from bridging an Ru–Ru bond to bridging the non-bonded Ru(1)…C(2) vector, i.e. formation of a thioether ligand has occurred. This reaction results in Ru(1) being attached to both sulfurs (Ru(1)–S(1,2) 2.365–2.486(6) Å). The four carbons of the C_4 chain are all attached to the Ru_5 core, but in this case, only three interact with Ru(4) in a π-bonded fashion (Ru–C 2.23–2.44(1) Å). Atom C(1) is strongly attached to the four basal Ru atoms (Ru(1,2,3,5)–C(1) 2.05–2.20(1) Å), while C(4) is also bonded to Ru(3) (2.21(1) Å). The minor isomer probably has the Ph and C≡CPh substituents on C(3) and C(4) interchanged, although only single isomers of the other complexes were characterised. The structure of **9** closely resembles that of the thiocarboxylato derivatives **11**, obtained from **1** and HC≡CR (R = Ph, $SiMe_3$) [3], although the SMe and PPh_2 groups bridging Ru(1)–Ru(2) and Ru(2)–Ru(3) have formally exchanged places.

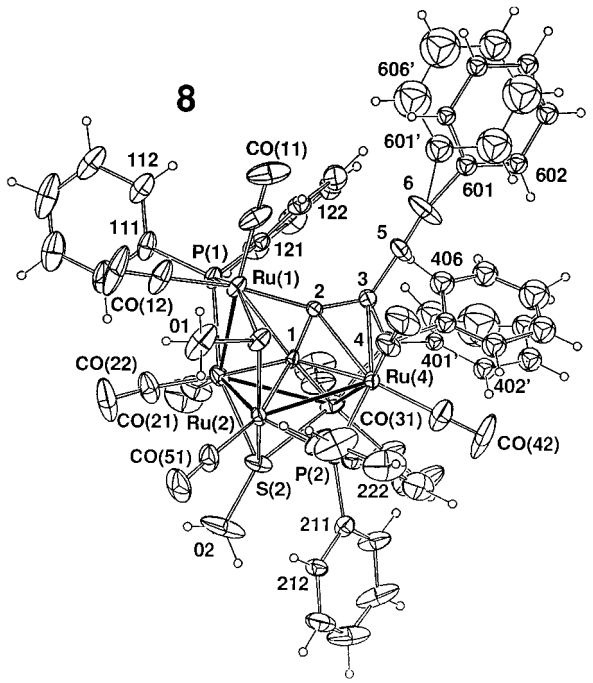

Fig. 1. Plots of a molecule of $Ru_5\{\mu_5\text{-}CC(C{\equiv}CPh)CPh\}(\mu_3\text{-}SMe)(\mu\text{-}SMe)(\mu\text{-}PPh_2)_2(CO)_9$ (**8**) showing the atom numbering scheme. In this and subsequent Figures, non-hydrogen atoms are shown as 20% thermal ellipsoids; hydrogen atoms have arbitrary radii of 0.1 Å.

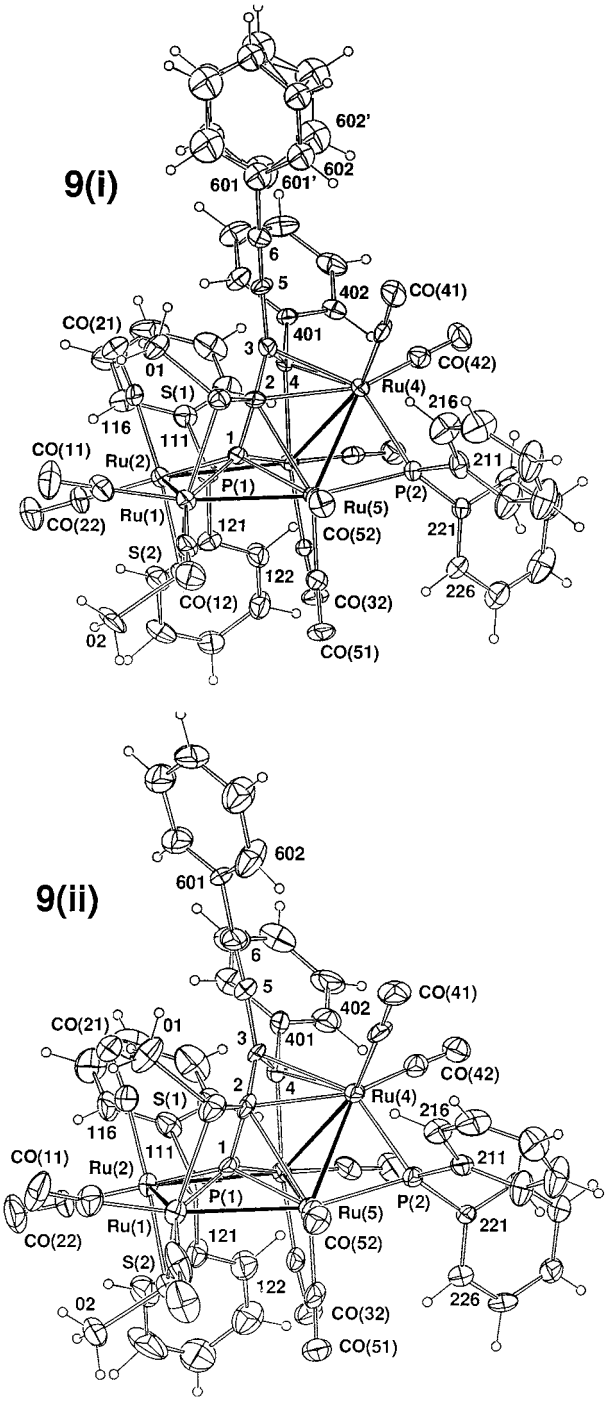

Fig. 2. (i), (ii) Plots of the two molecules of $Ru_5\{\mu_5\text{-}(CC\text{-}CPhC(C{\equiv}CPh)\}(\mu\text{-}SMe)_2(\mu\text{-}PPh_2)_2(CO)_{10}$ (**9**) showing the atom numbering scheme.

Perhaps of most interest is **10**, in which two diyne molecules have become attached to one carbon of the original C_2 ligand. The organic ligand in **10** is formed by addition of an inner carbon of one C≡C triple bond of each diyne to C(2). As in many reactions of **1**, this results in C(1) interacting more strongly with the Ru_4

base of the cluster (Ru(1,2,3,5)–C(1) 2.102–2.267(9) Å) [4]. In addition, we note that the organic ligand is on the obtuse face of the envelope, on the opposite side to the two μ_3-SMe groups. This contrasts with the situation in both **8** and **9**, where the organic ligand is held within the cavity formed by the Ru_3 flap and the Ru_4 rhombus. A consequence is that the two SMe groups adopt the μ_3 capping mode. Two five-membered metalladiene rings are formed: in one, all four carbons are involved in bonding to the cluster, with Ru(5) being π-bonded to C(1,2,3,4) (2.18–2.30(1) Å) and C(1,4) being σ-bonded to Ru(3) (2.102(9), 2.080(10) Å). The other RuC_4 ring, which is fused to the first by the shared C(1)–C(2) edge, is σ-bonded to Ru(1) (Ru(1)–C(1,6) 2.267(9), 2.05(1) Å), but C(5,6) forms a C=C double bond (1.40(1) Å) which remains uncoordinated. The whole ensemble forms a multi-branched C_{10} chain. The structure closely resembles that of **12**, obtained from **1** and $HC{\equiv}CSiMe_3$, which also contains two molecules of the mono-alkyne incorporated into the organic ligand, in this case also with a CO group and with one of the 1-alkynes apparently isomerised to the corresponding vinylidene before incorporation [3].

In all three complexes, the uncoordinated phenylethynyl substituents have the expected linear geometries, with angles at carbons of the C≡C triple bonds ranging between 168 and 178(1)° (except for C(6) in **8**, which is anomalously bent at 164(1)°). Separations between the triply-bonded carbons range between 1.11 and 1.19(1) Å.

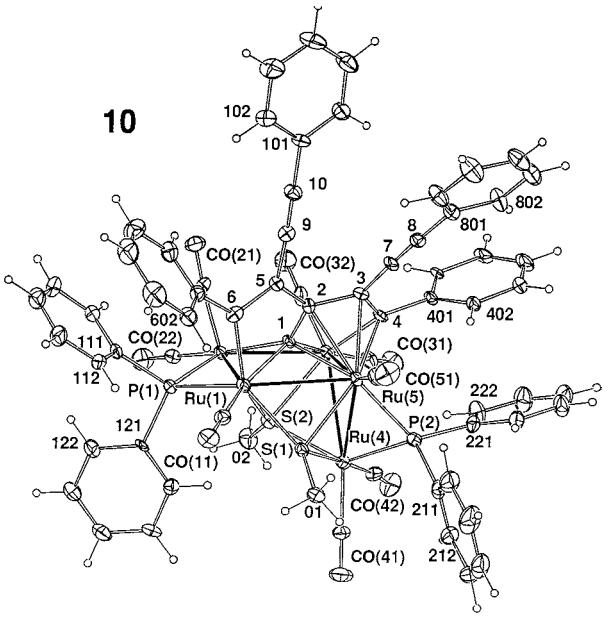

Fig. 3. Plots of a molecule of $Ru_5(\mu_4\text{-}CC\{C(C_2Ph)CPh\}C(C_2Ph)CPh)(\mu\text{-}PPh_2)_2(\mu_3\text{-}SMe)_2(CO)_8{\cdot}0.84CHCl_3$ (**10**) showing the atom numbering scheme.

Table 2
Selected bond parameters for **8** and **9**

	8	**9**
Bond lengths (Å)		
Ru(1)–Ru(2)	3.073(1)	2.792/2.792(2)
Ru(1)–Ru(5)	3.193(1)	2.838/2.844(2)
Ru(2)–Ru(3)	2.863(1)	2.903/2.878(2)
Ru(2)–Ru(5)	2.957(1)	
Ru(3)–Ru(4)	2.797(1)	2.850/2.847(2)
Ru(3)–Ru(5)		2.919/2.929(2)
Ru(4)–Ru(5)	2.911(1)	2.809/2.821(2)
Ru(1)–S(1)	2.412(3)	2.486/2.492(6)
Ru(1)–S(2)		2.365/2.346(6)
Ru(2)–S(2)	2.372(3)	2.397/2.396(4)
Ru(3)–S(2)	2.471(3)	
Ru(5)–S(1)	2.377(3)	
Ru(5)–S(2)	2.356(3)	
Ru(1)–P(1)	2.314(3)	
Ru(2)–P(1)	2.363(3)	2.257/2.262(5)
Ru(3)–P(1)		2.321/2.334(5)
Ru(4)–P(2)	2.334(2)	2.324/2.322(4)
Ru(5)–P(2)	2.195(3)	2.304/2.299(4)
Ru(1)–C(1)		2.05/2.05(1)
Ru(1)–C(2)	2.080(8)	
Ru(2)–C(1)	2.119(8)	2.19/2.15(2)
Ru(3)–C(1)	2.077(8)	2.20/2.14(1)
Ru(3)–C(4)	2.042(9)	2.21/2.17(2)
Ru(4)–C(1)	2.284(8)	
Ru(4)–C(2)	2.332(8)	2.44/2.40(1)
Ru(4)–C(3)	2.311(8)	2.23/2.23(1)
Ru(4)–C(4)	2.30(1)	2.27/2.25(2)
Ru(5)–C(1)	2.220(8)	2.09/2.11(1)
Ru(5)–C(2)		2.51/2.54(1)
S(1)–C(2)		1.79/1.79(1)
C(1)–C(2)	1.37(1)	1.42/1.47(3)
C(2)–C(3)	1.41(1)	1.47/1.46(2)
C(3)–C(4)	1.44(1)	1.42/1.44(2)
C(3)–C(5)	1.44(1)	1.43/1.44(2)
C(5)–C(6)	1.11(1)	1.15/1.13(3)
Bond angles (°)		
Ru(1)–S(1)–C(2)		80.4/80.3(6)
Ru(1)–C(1)–Ru(3)		146.0/147.8(9)
Ru(2)–C(1)–Ru(4)	155.6(4)	
Ru(2)–C(1)–Ru(5)		140.6/144.6(8)
Ru(3)–C(1)–Ru(5)	109.5(3)	
Ru(1)–C(1)–C(2)		107.0/104.8(9)
Ru(2)–C(1)–C(2)	129.7(6)	130.3/126.8(9)
Ru(3)–C(1)–C(2)	118.2(6)	105.9/106.5(8)
Ru(4)–C(1)–C(2)	74.7(5)	
Ru(5)–C(1)–C(2)	119.9(6)	89/89(1)
Ru(1)–C(2)–C(1)	87.8(5)	
Ru(3)–C(4)–C(3)	118.0(7)	112.0/112.3(9)
C(1)–C(2)–C(3)	114.4(7)	119/117(1)
C(2)–C(3)–C(4)	112.4(7)	114/114(1)
C(2)–C(3)–C(5)	126.2(9)	121/120(1)
C(4)–C(3)–C(5)	121.4(8)	
C(3)–C(5)–C(6)	174(1)	178/175(2)
Dihedral angles (°)		
For **8**	Ru(1,2,5)/Ru(2,3,5)	73.31(4)
	Ru(2,3,5)/Ru(3,4,5)	39.28(4)
For **9**	Ru(3,4,5)/Ru(1,2,3,5)	56.04(5)/57.92(5)

3. Discussion

The exposed location of the C_2 ligand in **1** makes it unusually susceptible to reactions with a variety of electrophiles [1]. Calculations have shown that electron density is concentrated on C(2) [5], so that it is not surprising to find that carbon electrophiles readily form new C–C bonds with this atom. Our previous papers [2–4] have described that a variety of terminal and disubstituted alkynes react at this point, and the complexes that we have isolated during this stage of the work have many similarities with those described earlier. The resulting organic ligands retain a high degree of unsaturation, which allows extended interaction with the metal clusters. In the course of these reactions, the atom C(1) is drawn into the Ru_4 rhombus which is present in the metal core.

Differences found in the reactions of **1** with the 1,3-diyne used here relate to formation of the thioether complex **9**, formed by migration of one on the μ-SMe groups in **1** to C(2). Unlike similar products from **1** and terminal alkynes [3], no CO is incorporated. Complex **10** is notable for containing two molecules of the 1,3-diyne, both of which have added to C(2) to give a multi-branched C_{10} chain.

The cluster valence electron (CVE) count expected for an M_5 cluster with six M–M bonds is 78 [6]. For these three complexes, this number is found for **9** [5Ru (40) + 10CO (20) + 2SMe (10) + $2PPh_2$ (6) + organic ligand (8)], but exceeded by **8** [5Ru (40) + 9CO (18) + (μ_3-SMe + μ-SMe) (8) + $2PPh_2$ (6) + organic ligand (8) = 80] and **10** [5Ru (40) + 8CO (16) + 2SMe (10) + $2PPh_2$ (6) + organic ligand (8) = 80]. Detailed examination of the Ru–Ru separations in each complex shows that in **9**, all fall in the range 2.792–2.919(2) Å (av. 2.852 Å). In **8** and **10**, there are two longer Ru–Ru separations that exceed 3.0 Å, the remaining four being between 2.797–2.957(1) and 2.829–2.972(1) Å, respectively, with averages for all Ru–Ru distances of 2.966 and 2.935 Å.

These long M–M separations are characteristic of a growing number of metal clusters containing bridging phosphorus and sulfur ligands. The explanation in terms of occupancy of low-lying LUMOs, which are largely M–M anti-bonding in character, by the extra electrons which leads to lengthening of two or more M–M bonds, rather than cleavage of one M–M bond, has been discussed elsewhere [7].

Table 3
Selected bond parameters for **10**

Bond lengths (Å)			
Ru(1)–Ru(2)	2.890(1)	Ru(2)–C(1)	2.12(1)
Ru(1)–Ru(5)	3.034(1)	Ru(3)–C(1)	2.102(9)
Ru(2)–Ru(3)	2.854(1)	Ru(3)–C(4)	2.08(1)
Ru(3)–Ru(4)	3.038(2)	Ru(5)–C(1)	2.179(9)
Ru(3)–Ru(5)	2.829(1)	Ru(5)–C(2)	2.30(1)
Ru(4)–Ru(5)	2.972(1)	Ru(5)–C(3)	2.26(1)
Ru(1)–S(1)	2.361(3)	Ru(5)–C(4)	2.30(1)
Ru(2)–S(2)	2.407(3)	C(1)–C(2)	1.39(1)
Ru(3)–S(2)	2.402(3)	C(2)–C(3)	1.44(1)
Ru(4)–S(1)	2.383(3)	C(2)–C(5)	1.47(1)
Ru(4)–S(2)	2.429(3)	C(3)–C(4)	1.48(1)
Ru(5)–S(1)	2.370(3)	C(3)–C(7)	1.43(1)
Ru(1)–P(1)	2.222(3)	C(7)–C(8)	1.19(1)
Ru(2)–P(1)	2.288(3)	C(8)–C(801)	1.44(2)
Ru(4)–P(2)	2.321(3)	C(5)–C(6)	1.40(1)
Ru(5)–P(2)	2.345(3)	C(5)–C(9)	1.42(1)
Ru(1)–C(1)	2.267(9)	C(9)–C(10)	1.17(2)
Ru(1)–C(6)	2.05(1)	C(10)–C(101)	1.44(2)
Bond angles (°)			
Ru(1)–C(1)–Ru(3)	140.8(5)	C(2)–C(3)–C(7)	123.3(9)
Ru(2)–C(1)–Ru(5)	144.0(5)	C(4)–C(3)–C(7)	122.7(9)
Ru(1)–C(1)–C(2)	95.6(6)	C(2)–C(5)–C(6)	114.9(9)
Ru(2)–C(1)–C(2)	138.0(7)	C(2)–C(5)–C(9)	119.4(9)
Ru(3)–C(1)–C(2)	117.9(7)	C(6)–C(5)–C(9)	125.5(9)
Ru(5)–C(1)–C(2)	76.9(6)	C(3)–C(7)–C(8)	178(1)
Ru(1)–C(6)–C(5)	109.1(7)	C(7)–C(8)–C(801)	178(1)
C(1)–C(2)–C(3)	112.8(9)	C(5)–C(9)–C(10)	177(1)
C(1)–C(2)–C(5)	120.9(9)	C(9)–C(10)–C(101)	178(1)
C(2)–C(3)–C(4)	114.0(9)		
Dihedral angle (°)			
Ru(3,4,5)/Ru(1,2,3,5)	87.71(3)		

4. Conclusions

Reactions of **1** with the 1,3-diyne PhC≡CC≡CPh have given products largely analogous to those obtained from other reactions of **1** with mono-alkynes and occur by addition of a carbon of one C≡C triple bond to one carbon of the C_2 ligand in **1**. In one product, addition of two molecules of the diyne to the same carbon of the C_2 ligand produces a multi-branched C_{10} chain. It would appear that the C_2 ligand behaves as a permetallated alkyne in these reactions, which proceed by insertion of the C≡C triple bond of the entering alkyne into an Ru–C bond. In this sense, these reactions are not models of possible reactions of C_2 fragments on metal surfaces to give straight-chain hydrocarbons.

5. Experimental

5.1. General conditions

All reactions were carried out under dry, high-purity nitrogen using standard Schlenk techniques. Solvents were dried and distilled before use. Elemental analyses were carried out by the Canadian Microanalytical Service, Delta, BC, Canada V4G 1G7. TLC was carried out on glass plates (20 × 20 cm) coated with silica gel (Merck 60 GF_{254}, 0.5 mm thick).

Table 4
Crystal data and refinement details for complexes **8**, **9** and **10**

Compound	**8**	**9**	**10**
Formula	$C_{53}H_{36}O_9P_2Ru_5S_2$	$C_{54}H_{36}O_{10}P_2Ru_5S_2 \cdot 0.39CHCl_3$	$C_{68}H_{46}O_8P_2Ru_5S_2 \cdot 0.84CHCl_3$
MW	1448.3	1522.5	1722.7
$F(000)$	2832	5955.6	3395
Crystal system	Monoclinic	Monoclinic	Monoclinic
Space group	$P2_1/c$	$P2_1/c$	$P2_1/c$
a (Å)	10.891(4)	23.084(6)	20.682(14)
b (Å)	17.959(6)	21.468(2)	19.874(4)
c (Å)	27.799(12)	24.772(3)	16.676(4)
b (°)	99.72(3)	114.96(2)	97.46(5)
V (Å^3)	5359	11129	6796
Z	4	8	4
D_c (g cm^{-3})	1.79	1.82	1.68
Crystal size (mm)	$0.45 \times 0.13 \times 0.18$	$0.36 \times 0.19 \times 0.26$	$0.80 \times 0.14 \times 0.14$
A^* (min, max)	1.21, 1.31	1.18, 1.36	1.17, 1.22
μ (cm^{-1})	15.3	15.5	13.2
N	9406	19569	10589
N_o	5534	9729	6476
R	0.049	0.066	0.052
R_w	0.047	0.062	0.054

5.2. Reagents

Complex **1** [8] and PhC_2C_2Ph [9] were prepared by the cited methods. CO (BOC) was used as received.

5.3. Instrumentation

IR: Perkin–Elmer 1700X FTIR; 683 double beam, NaCl optics; NMR: Bruker CXP300 or ACP300 (^{1}H-NMR at 300.13 MHz, ^{13}C-NMR at 75.47 MHz); samples dissolved in $CDCl_3$. FAB MS: VG ZAB 2HF (FAB MS, using 3-nitrobenzyl alcohol as matrix, exciting gas Ar, FAB gun voltage 7.5 kV, current 1 mA, accelerating potential 7 kV).

5.4. Reactions of *1* with 1,4-diphenylbuta-1,3-diyne

5.4.1. At 90°C for 9.5 h

A solution of **1** (80 mg, 0.061 mmol) and 1,4-diphenylbutadiyne (50 mg, 0.25 mmol) in toluene (10 ml) in a Carius tube was heated for 9.5 h at 90°C. After cooling to room temperature (r.t.) the solvent was removed and the residue purified by preparative TLC (10:3 light petroleum–acetone) to yield four bands. A dark brown band (R_f 0.3) was recrystallised from CH_2Cl_2/MeOH to yield $Ru_5\{\mu_5\text{-}(CCCPhC(C{\equiv}CPh)\}(\mu\text{-}SMe)_2(\mu\text{-}PPh_2)_2(CO)_{10}$ (**7**) (22 mg, 24%). A red band (R_f 0.4) was recrystallised from CH_2Cl_2/MeOH to yield $Ru_5\{\mu_5\text{-}CCCCPh(C_2Ph)\}(\mu\text{-}PPh_2)_2(\mu\text{-}SMe)(\mu_3\text{-}SMe)\text{-}(CO)_{11}$ (**6**) (22 mg, 24%). An orange band (R_f 0.5; 30 mg) contained a mixture of $Ru_5\{\mu_5\text{-}CCCPhC\text{-}(C{\equiv}CPh)\}(\mu_3\text{-}SMe)(\mu\text{-}SMe)(\mu\text{-}PPh_2)_2(CO)_9$ (**8**) (17 mg, 19%) and $Ru_5\{\mu_5\text{-}CC(SMe)C(C{\equiv}CPh)CPh\}(\mu\text{-}SMe)(\mu\text{-}PPh_2)_2(CO)_{10}$ (**9**) (13 mg, 14%). Some starting material was also recovered (R_f 0.6; 11 mg, 14%).

5.4.2. At 90°C for 43 h

A solution of **1** (75 mg, 0.058 mmol) and 1,4-diphenylbutadiyne (50 mg, 0.25 mmol) in toluene (10 ml) in a Carius tube was heated for 43 h at 90°C. After cooling to r.t. the solvent was removed and the residue purified by preparative TLC (10:3 light petroleum–acetone) to yield four bands. An orange band (R_f 0.5; 31 mg) contained a mixture of **8** (18 mg, 21%) and **9** (13 mg, 15%). A brown band (R_f 0.4) was further purified by preparative TLC (4:1 light petroleum–CH_2Cl_2) to yield two fractions. A red band (R_f 0.40) was recrystallised from CH_2Cl_2–MeOH to yield **6** (4 mg, 5%). A brown band (R_f 0.35) was recrystallised from CH_2Cl_2–MeOH to yield $Ru_5\{\mu_4\text{-}CC\{C(C{\equiv}CPh)CPh\}C(C{\equiv}CPh)\text{-}CPh\}(\mu_3\text{-}SMe)_2(\mu\text{-}PPh_2)_2(CO)_8$ (**10**) (12 mg, 13%). A dark brown band (R_f 0.3) was recrystallised from CH_2Cl_2/MeOH to yield **7** (30 mg, 35%). A minor black band (R_f 0.25; 4 mg) was not identified.

5.4.3. At 120°C for 12 h

A solution of **1** (47 mg, 0.036 mmol) and 1,4-diphenylbutadiyne (80 mg, 0.40 mmol) in toluene (10 ml) in a Carius tube was heated for 8 h at 120°C. After cooling to r.t. the solvent was removed and the residue purified by preparative TLC (10:3 light petroleum–acetone) to yield two major bands. An orange band (R_f 0.65) was further purified by preparative TLC (4:1 light petroleum–CH_2Cl_2) to yield two bands. A red band (R_f 0.50) was recrystallised from CH_2Cl_2–MeOH to yield two isomers (4:1) of **9** (10 mg, 19%). A light brown band (R_f 0.45) was recrystallised from CH_2Cl_2–MeOH to yield **8** (12 mg, 23%). The second brown band (R_f 0.65), from the initial purification, was recrystallised from CH_2Cl_2/MeOH to yield **7** (27 mg, 51%).

5.5. Crystallography

Unique data sets were measured at ca. 295 K to the limit $2\theta_{max} = 50°$ using an Enraf–Nonius CAD4 diffractometer ($2\theta/\theta$ scan mode; monochromatic Mo–K_α radiation, $\lambda = 0.7107_3$ Å); N independent reflections were obtained, N_o with $I > 3\sigma(I)$ being considered 'observed' and used in the full-matrix least-squares refinement after Gaussian absorption correction. Anisotropic thermal parameters were refined for the non-hydrogen atoms; $(x, y, z, U_{iso})_H$ were included constrained at estimated values. Conventional residuals R, R' on $|F|$ are quoted, statistical weights derivative of $\sigma^2(I) = \sigma^2(I_{diff}) + 0.0004\sigma^4(I_{diff})$ being used. Computation used the XTAL 2.6 program system [10] implemented by S.R. Hall; neutral atom complex scattering factors were employed. Pertinent results are given in the Figures and Tables.

5.6. Abnormal features/variations in procedure

(**8**). The two phenyl rings on the Ph_2C_6 ligand were modelled as disordered over two sets of sites, occupancies set at 0.5 after trial refinement, the components associated with ring 60 being refined as rigid bodies. Although most evident thus, 'thermal motion' throughout the whole molecule was rather high and may be indicative of propagation of the disorder to a significant extent throughout the lattice. Alternatively, it may be indicative of more subtle variations in bonding modes or unresolved space group ambiguity.

(**9**). Phenyl ring 60 of molecule **1** was modelled as disordered over two sets of sites, occupancies set at 0.5 after trial refinement. The chloroform solvent occupancy refined to 0.774(6).

(**10**). The chloroform molecule was refined with constrained geometry and the carbon thermal parameter form isotropic, site occupancy refining to 0.838(8).

6. Supplementary material

Crystallographic data for the structural analysis have been deposited with the Cambridge Crystallographic Data Centre, CCDC nos. 118288–118290 for compounds **8**, **9** and **10**, respectively. Copies of the information can be obtained free of charge from The Director, CCDC, 12 Union Road, Cambridge CB2 1EZ, UK (Fax: + 44-1223-336-033; e-mail: deposit@ccdc.cam.ac.uk or www: http://www.ccdc.cam.ac.uk).

Acknowledgements

We thank the Australian Research Council for financial support and Johnson Matthey Technology Centre for a generous loan of $RuCl_3 \cdot nH_2O$.

References

[1] (a) M.I. Bruce, J. Clust. Sci. 8 (1997) 293. (b) M.I. Bruce, Coord. Chem. Rev. 166 (1997) 91.
[2] C.J. Adams, M.I. Bruce, B.W. Skelton, A.H. White, J. Chem. Soc. Dalton Trans. (1999) 1283.
[3] C.J. Adams, M.I. Bruce, B.W. Skelton, A.H. White, J. Chem. Soc. Dalton Trans. (1999) 2451.
[4] C.J. Adams, M.I. Bruce, B.W. Skelton, A.H. White, J. Organomet. Chem. 584 (1999) 254.
[5] G. Frapper, J.-F. Halet, M.I. Bruce, Organometallics 16 (1997) 2590.
[6] D.M.P. Mingos, A.S. May, in: D.F. Shriver, H.D. Kaesz, R.D. Adams (Eds.), The Chemistry of Metal Cluster Complexes, VCH, New York, Ch. 2, 1990.
[7] N. Lugan, P.-L. Fabre, D. de Montauzon, G. Lavigne, J.-J. Bonnet, J.-Y. Saillard, J.-F. Halet, Inorg. Chem. 32 (1993) 1363.
[8] C.J. Adams, M.I. Bruce, B.W. Skelton, A.H. White, J. Chem. Soc. Dalton Trans. (1997) 2937.
[9] I.D. Campbell, G. Eglinton, Org. Synth. Coll. 5 (1973) 517.
[10] S.R. Hall, J.M. Stewart (Eds.), XTAL Users' Manual, Version 2.6', Universities of Western Australia and Maryland, 1989.